

3D small-gain formula allowing strong focusing and harmonic lasing for a ring-based x-ray free electron laser oscillator

Li Hua Yu[✉], Victor Smaluk, Timur Shaftan, Ganesh Tiwari[✉], and Xi Yang
NSLS-II, Brookhaven National Laboratory, New York 11973, USA

 (Received 25 October 2023; accepted 3 June 2024; published 21 June 2024)

We present a detailed derivation of a formula for the small-gain calculation for an x-ray free electron laser oscillator (XFEL) based on a medium-energy (3–4 GeV) storage ring. We found harmonic lasing and strong focusing are essential for this beam energy range. Taking the small-signal low-gain formula developed by Kim and his colleagues, we modified it in such a way that the gain can be calculated without the “no focusing approximation,” and a strong focusing can be applied, as well as harmonic lasing. In this formula, the gain is represented as a product of two factors with one of them depending only on the harmonic number, undulator period, and gap. Using this factor, we show that it is favorable to use harmonic lasing to achieve hard x-ray FEL working in the small-signal low-gain regime with the medium-energy electron beam. Our formula also allows FEL optimization by varying the vertical gradient of the undulator, the vertical dispersion, and the horizontal and vertical focusing, independently. As an example, we applied this formula to study the feasibility of an XFEL option for the National Synchrotron Light Source II (NSLS-II) upgrade. Since a quite high peak current is required for the FEL, collective effects of beam dynamics in medium-energy synchrotrons significantly affect the electron beam parameters. We carried out a multiparameter optimization taking collective effects into account. Note, even though our example is for a ring-based XFEL at 3 to 4 GeV, the formula and, in particular, the approach developed here may be applied to other types of FELs.

DOI: [10.1103/PhysRevAccelBeams.27.060702](https://doi.org/10.1103/PhysRevAccelBeams.27.060702)

I. INTRODUCTION

We present a more detailed derivation of the small-gain formula for a ring-based x-ray free electron laser oscillator (XFEL), published in the proceedings of IPAC2021 [1]. An x-ray FEL oscillator (XFEL) based on a transverse gradient undulator (TGU) [2–4] considered by the APS and SLAC collaboration [5,6] provides a promising direction for a storage-ring-based fully coherent hard x-ray source. The difficulty associated with the relatively large energy spread of 10^{-3} in the storage ring is mitigated by introducing TGU and dispersion in the FEL by a trade-off with increased transverse beam size.

The examples in the above references are for the electron beam energy of 6 GeV. For a medium-energy light source such as NSLS-II operated at 3 GeV, the first difficulty is the relatively lower beam energy. To achieve a hard x-ray with 0.12 nm wavelength, an undulator period of less than 1 cm and a gap of a few millimeters are required to satisfy the resonance condition, which makes it very difficult to

achieve the required electron beam quality. Under this circumstance, we are obliged to consider harmonic lasing.

Our motivation for developing a gain formula with harmonic lasing and strong focusing is that we found these features necessary for XFEL in a lower energy range of 3–4 GeV. As a result, we need to justify the need for harmonic lasing and strong focusing here in the Introduction. The formula about 1D gain relation with the undulator period λ_u , field parameter K , and gap is indeed simple, but the conclusion about the need to consider harmonic lasing is by no means obvious because we need to compare gain in detail: as far as we know, many hard x-ray FELs in the world including those being developed now are all using fundamental lasing without optimization of harmonic number. We think if this optimization procedure is applied, it may help to lower the cost of future XFELs and also help to relax the requirements on the electron beam. In fact, we note here that the method considered here is not only applied to XFEL in 3 to 4 GeV storage rings as in the case we discussed in this paper, it may also be extended to XFEL based on superconducting linacs, it may also be applied to XFELs with higher energy and even shorter wavelengths XFELs to relax some stringent requirements on undulator and electron beam parameters. The Maxwell-Vlasov equations with harmonic lasing and strong focusing included may be incorporated into the high-gain FEL formula and applied

Published by the American Physical Society under the terms of the Creative Commons Attribution 4.0 International license. Further distribution of this work must maintain attribution to the author(s) and the published article's title, journal citation, and DOI.

to high-gain XFEL too. Without detailed gain calculation, it is not clear whether or how much we can benefit from the inclusion of harmonic lasing and strong focusing. Thus, we are justified to give a more quantitative study of their effects.

In this paper, we use a 3 to 4 GeV XFEL as an example to study the possibility of harmonic lasing and strong focusing because, on the one hand, one of our motivations is to study whether it is possible to have an XFEL as an option for NSLS-II upgrade, on the other hand, the main advantage of XFEL is a combination of the synchrotron and FEL capabilities and no need for a very expensive superconducting linac. A storage ring FEL [7–9] can operate at a high repetition rate (in the order of several MHz range). Another advantage is that the single-pulse energy of the storage ring x rays is higher because the pulse is longer (10 ps as compared to 100 fs of high-gain FELs). The electron beam in a storage ring is extremely stable because of the use of advanced orbit feedback. Storage rings operate with a constant beam intensity provided by top-off injection, so the pulse-to-pulse fluctuations are small. Note that the harmonic lasing gain formula derived here is also valid for a low-energy linac-based XFEL, hence even though in this paper, our example is limited to XFEL, the method may be applied to other types of XFELs.

The harmonic generation and harmonic lasing, for high gain FEL, are analyzed, for example, in [10,11]. However, we need more quantitative analysis of the scaling relation, particularly because we are considering the case of lower energy and large energy spread. We adopt the approach in Refs. [5,6] for the low gain formula which is based on the low gain formula derived by Kim [12]. For this purpose, we need to follow through with the gain derivation to explicitly allow for harmonic lasing without taking the “no focusing” approximation. Before going into more detailed analysis, we first consider the gain formula in 1D Madey theorem with harmonic number h and when energy spread is negligible; the FEL gain can be cast in a form convenient for scaling with harmonic number h and undulator period λ_u as follows:

$$G_{1D} = \left(\frac{hK^2 [JJ]_h^2}{\lambda_u} \right) \left(\pi^2 \frac{I L_u^3}{I_A \gamma^3 \Sigma} \right) \left(\frac{d}{d\Phi} \left(\frac{\sin \Phi}{\Phi} \right)^2 \right), \quad (1)$$

where K is the undulator parameter given by the peak field B_{peak} in the resonance condition

$$\lambda_s = \frac{\lambda_u}{2\gamma_0^2} \left(1 + \frac{K^2}{2} \right). \quad (2)$$

Here γ_0 is the resonant electron beam energy in the unit of electron rest mass, λ_s is the FEL wavelength, $L_u = N_u \lambda_u$ is the undulator length with the number of period N_u . $[JJ]_h = (-1)^{(h-1)/2} [J_{(h-1)/2}(\frac{hK^2}{4+2K^2}) - J_{(h+1)/2}(\frac{hK^2}{4+2K^2})]$ is

the Bessel function factor, $\Sigma = 2\pi\sigma_x\sigma_y$ is the electron beam cross-section area with rms sizes σ_x and σ_y , and I is beam peak current. $I_A = 4\pi mc^3 \epsilon_0 / e \approx 17$ kA is the Alfvén current. $\Phi = \pi\Delta\nu N_u - 2\eta h\pi N_u$ is the phase advance in the undulator due to detuning, with $\eta = (\gamma - \gamma_0)/\gamma_0$ being the relative energy detuning of mean energy γ from resonance, $\Delta\nu = h(\omega - \omega_s)/\omega_s$ the laser frequency detuning from resonance frequency $\omega_s = 2\pi/\lambda_s$ with harmonic number h .

The beam energy spread effect on the 1D gain given by Eq. (1) can be estimated by averaging the third term $\frac{d}{d\Phi} \left(\frac{\sin \Phi}{\Phi} \right)^2$ over the energy space spanned by the beam.

For a given wavelength λ_s , energy γ , peak current I , undulator length L_u , and the electron beam cross section Σ , the second factor is constant. Although the 1D gain is directly proportional to the ratio of harmonic number to undulator period, the need to increase the harmonic number h becomes clear only after we calculate the first factor $\left(\frac{K^2 [JJ]_h^2}{\lambda_u} \right)$ as a function of h and λ_u while taking into account the resonance condition [Eq. (2)] and the relation of undulator parameter K to the undulator period λ_u , peak field B_{peak} , and gap g . Assuming the relation between B_{peak} and g is given by the Halbach formula [13] for rare earth cobalt magnets, we have

$$K = \frac{e\lambda_u B_{\text{peak}}}{2\pi mc} = 93.43\lambda_u [\text{m}] B_{\text{peak}} [\text{T}],$$

$$B_{\text{peak}} = 3.33 \exp \left(-5.47 \frac{g}{\lambda_u} + 1.8 \left(\frac{g}{\lambda_u} \right)^2 \right). \quad (3)$$

For a given λ_u and h , the resonance condition [Eq. (2)] determines K , then Eq. (3) determines B_{peak} and the gap g . For a 3 GeV beam, and for $\lambda_s = 0.12$ nm, we plot $\frac{K^2 [JJ]_h^2}{\lambda_u}$ as a function of λ_u for $h = 1, 5$, respectively, in Fig. 1(a). We plot the gap g and K , respectively, in Fig. 1(b) and Fig. 2(a) as function of λ_u for $h = 1$ and $h = 5$. From Fig. 1(b), we see that the range of period to satisfy the resonance condition is between 4.5 and 8.2 mm for $h = 1$. At 4.5 mm, the gap is zero while at the other limit 8.2 mm, the gap is 5.5 mm, but K approaches zero in Fig. 2(a). For $h = 5$, the range satisfying the resonance condition is above 9.2 mm, and the gap is above 7 mm when $\lambda_u > 2.2$ cm. The narrow gap makes it a tough choice to realize a Sm-Co based undulator for the first harmonic FEL; from this point of view of gap alone, we would need to consider the possibility of higher harmonics.

The main issue here is whether there is sufficient gain with $h > 1$, i.e., whether the single-pass FEL gain is larger than the total power loss of the x-ray cavity in a round trip. We considered a bow-tie configuration with a 200 m roundtrip and the cavity consists of four crystals and two focusing lenses as identified in Fig. (3) of Ref. [14]. To estimate power loss and out-coupling through the cavity,

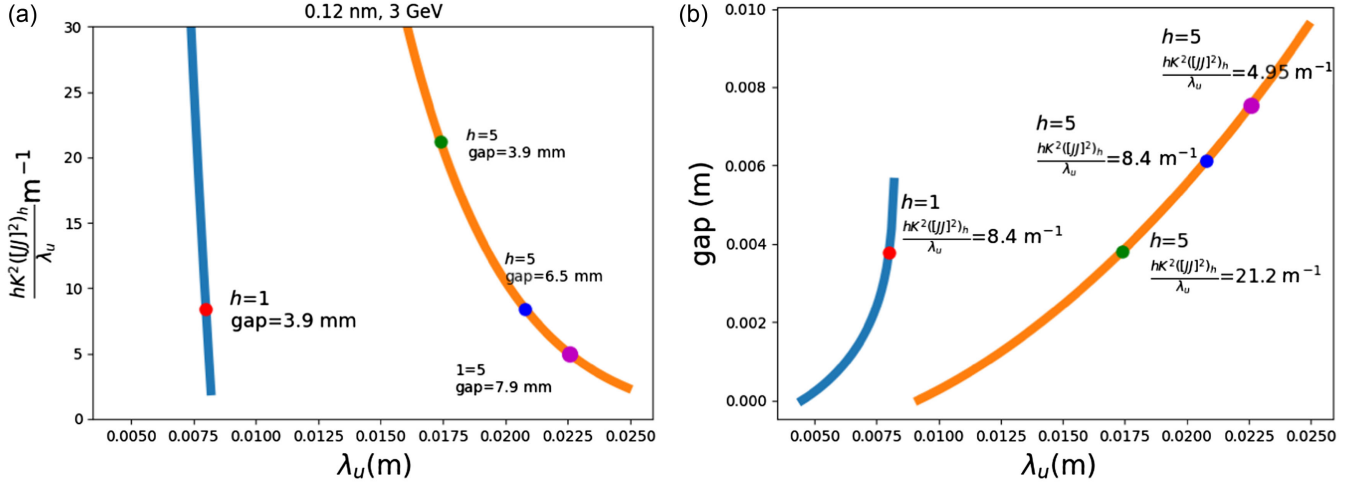


FIG. 1. (a) $\frac{K^2[JJ]_h^2 h}{\lambda_u}$ vs λ_u , compare $h = 5$ with $h = 1$, showing the advantage of higher h . We compare two points with the same gap of $g = 3.9$ mm, the first factor is 8.4 for $h = 1$, while it is 21.2 for $h = 5$, even though this gap is too narrow to be practical. Another pair of points has the same gain factor $\frac{K^2[JJ]_h^2 h}{\lambda_u} = 8.4$, the gap is 3.9 mm for $h = 1$, while for $h = 5$, the gap is 6.1 mm. (b) Gap vs λ_u .

we considered a monochromatic radiation beam at 0.12 nm with a Gaussian transverse profile in physical and angular space expected at the steady-state XFEL. Since angular filtering from Bragg-crystal in the reflecting plane dominates power loss in the cavity, we stabilized cavities under consideration by placing two Be lenses [15] with the same focal length at either side of the undulator. The first lens after the undulator collimates the diverging radiation beam ensuring a parallel transverse profile of the radiation beam while propagating through all crystals before the second lens; the second lens then focuses the radiation beam at the undulator center. Our analysis for monochromatic x rays indicates highly transmissive Be refractive lenses with focal lengths greater than 1 m are feasible for hard x rays [16]. We further confined crystal choices to symmetrical Bragg reflection cases for simplicity and convenience and then identified a few diamond Bragg crystals with very low power losses. Our studies and the recent SLAC and ANL articles [17–20] show the loss in each mirror is less than 1% and two compound-refractive lenses (CRL) together contribute less than 0.25% loss for focal lengths greater than or equal to 20 m if the effective aperture of the CRL is bigger than 3 times the rms size of the x-ray beam at the steady state [16]. So, the total power loss in the optical cavity is less than 4.5% and we can consider out-coupling up to 0.5%, then the total cavity loss including out-coupling is less than 5%. As a result, we set the lower limit of the required FEL gain to 6% to get some margin above the lasing limit of 5%.

First, we consider the factor $\frac{K^2[JJ]_h^2 h}{\lambda_u}$ in the 1D gain. Figure 1(a) shows the advantage of higher h . The examples show for the contribution to the first factor, for the same gap, a higher harmonic number has a higher gain, while for the same gain, a higher harmonic number has a larger gap. The magenta points in Figs. 1

and 2 are the working points we use in the following sections.

However, the contribution from the third factor $\frac{d}{d\Phi} \left(\frac{\sin\Phi}{\Phi} \right)^2$ is more complicated. With a maximum of 0.54 at $\Phi = -1.3$, the term $2\eta h\pi N_u = 2\eta\pi L_u \frac{h}{\lambda_u}$ in Φ has a spread proportional to h/λ_u . After averaging over energy spread σ_η , the increased spread would reduce the average value of the third factor. To see its effect on the spread of Φ , we plot h/λ_u as a function of λ_u in Fig. 2(b). For the pair of points in Fig. 1(a) with the same first gain factor 8.4, we see the ratio $\frac{h}{\lambda_u}$ increases from 1.2 for $h = 1$ to 2.6 for $h = 5$. This reduction is significant, hence the main question in the following discussion is whether the gain reduction due to the large energy spread can be mitigated by TGU and dispersion sufficiently to maintain the required gain.

In the formulation developed in [5,6,12] about the 3D gain, if we assume the gradient is in the vertical direction, then the undulator parameter $K = K_0(1 + \alpha y)$, the energy is $\gamma = \gamma_0(1 + \eta)$, for $\alpha y \ll 1, \eta \ll 1$, the resonance condition becomes

$$\begin{aligned} \lambda &= \frac{\lambda_u}{2\gamma^2 h} \left(1 + \frac{K^2}{2} \right) \\ &= \frac{\lambda_u}{2\gamma_0^2 h} \frac{1 + \frac{K_0^2}{2}(1 + \alpha y)^2}{(1 + \eta)^2} \\ &\approx \frac{\lambda_u}{2\gamma_0^2 h} \left(1 + \frac{K_0^2}{2} \right) \left(1 + \frac{2K_0^2}{2 + K_0^2} \alpha y - 2\eta \right). \end{aligned} \quad (4)$$

If we assume the dispersion D is in the vertical direction, the vertical distribution in Gaussian takes the form $\exp\left(-\frac{(y-D\eta)^2}{2\sigma_y^2}\right)$. The centroid of the electron beam with energy η is shifted to $D\eta$. For small σ_y , $y \approx D\eta$ and the

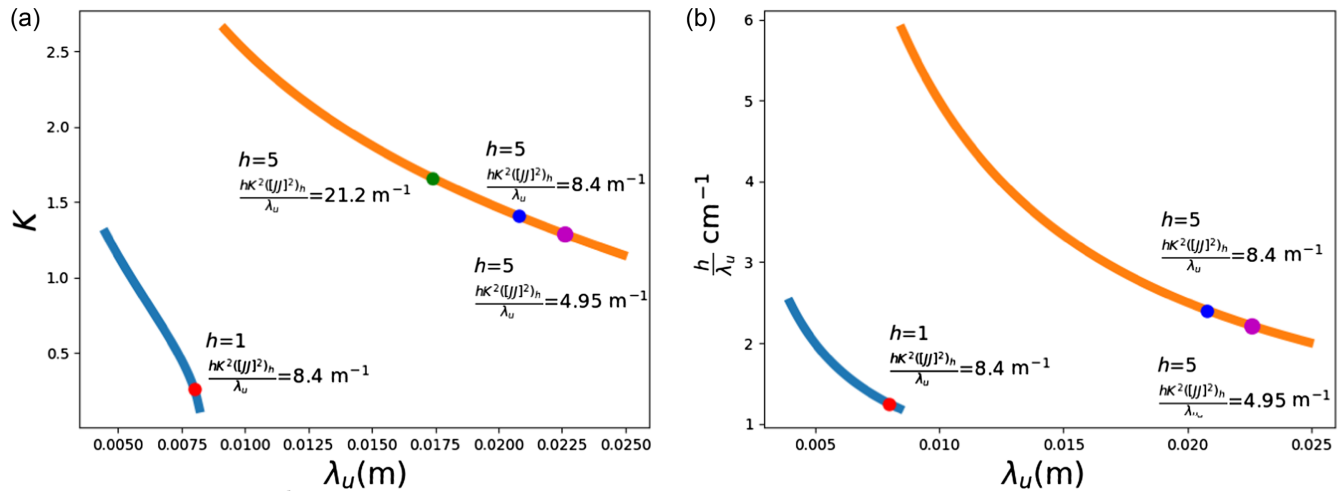


FIG. 2. (a) K vs λ_u , (b) $\frac{h}{\lambda_u}$ vs λ_u . For the pair of points in Fig. 1(a) with the same first gain factor 8.4, we see the ratio $\frac{h}{\lambda_u}$ increases from 1.2 for $h = 1$ to 2.6 for $h = 5$.

deviation from the resonance condition due to the spread in η is given by $\frac{2K_0^2}{2+K_0^2}\alpha D\eta - 2\eta$. If $\alpha D = \frac{2+K_0^2}{K_0^2}$, then the gain reduction due to large energy spread is mitigated. However, there is a trade-off with increased vertical beam size. The term $\frac{2K_0^2}{2+K_0^2}\alpha\sigma_y$ causes a deviation from resonance condition in Eq. (4) and $D\sigma_y$ increases the transverse beam cross section Σ in the gain formula [Eq. (1)]. Both effects reduce the gain and both are determined by the emittance and focusing in the undulator.

To study the beam quality required for an x-ray FEL working in the medium energy range, we apply the gain formula developed by Kim [12] for optimization, with the 3D effect of diffraction, beam divergence, and betatron motion taken into account, and in particular, with addition to include harmonic lasing. We note that the “brightness function” based gain formula was obtained with “no focusing” approximation in Ref. [12] and extended to the TGU case for fundamental radiation [5,6]. The no focusing approximation essentially neglects the undulator or external beam focusing effect. We realized that nonzero focusing was required to optimize the gain with TGU for harmonic lasing. During the optimization, we often arrived at parameters that violated the no focusing approximation. Hence, it is desirable to develop an approach to calculate the gain without taking the no focusing approximation. In this paper, we present a derivation of the gain formula without taking the no focusing approximation and some examples of the required parameters for a medium energy storage ring such as NSLS-II.

In the following, we present a derivation of the gain formula with harmonic lasing and without taking the no focusing approximation, and some examples of the required parameters for a medium energy storage ring such as NSLS-II. In Sec. II, we first follow [12] to describe the general 3D gain formula that resembles 1-D Madey theorem, Eq. (23)

in [12]. This general gain formula is our starting point, which is also the last step in [5,6,12] right before taking the no focusing approximation. Although the equation does not require a specific distribution, below we use a Gaussian beam because it allows us to solve the equation analytically. Then in Sec. III, we consider a focusing lattice interlaced with the undulator, the system has nearly constant beta and dispersion functions and hence has nearly constant transverse beam profile in the undulator, this allows us to carry out a multivariable Gaussian integration without taking the no focusing approximation and reduce the gain formula to a double integral, similar to the result of [5,6,12]. In Sec. IV, we present some examples of gain optimization using the formula to study the required parameters for an x-ray FEL oscillator in a medium energy storage ring such as the upgrade being considered at the NSLS-II. In Sec. V, we carry out gain optimization with collective effects taken into account. The result indicates the feasibility of XFEL for a 3 GeV storage ring at NSLS-II. In Appendix A, in order to clarify the notations in this paper and in particular to include the harmonic number h in the formulation, we briefly describe the steps that lead to the general 3D gain formula in Sec. I, starting from the combined Maxwell-Vlasov equations.

II. GAIN FORMULA

The gain in small signal, low-gain regime taking into account the 3D effect of diffraction, beam divergence, and betatron motion, is given in the following Eq. (5), which is Eq. (23) of [12], with a minor elaboration of introducing the transverse gradient and dispersion for TGU as in [5,6]. For convenience, we adopt nearly identical notation as [12], with only a few exceptions to unite with the notations in [5,6,12] and the notations we used in the early development of the coupled Maxwell-Vlasov equations for high-gain FEL [21–24]. The gain expression has multiple integrations to be carried out for application as given by

$$G = -c_h \frac{\int d\eta d\mathbf{x} d\mathbf{p} \bar{F}(\mathbf{x}, \mathbf{p}, \eta; 0) \frac{\partial}{\partial \eta} \left| \int d\phi A_\nu^{(0)}(\phi, 0) U_\nu^*(\eta, \phi, \mathbf{p}, \mathbf{x}) \right|^2}{\int |A_\nu^{(0)}(\phi)|^2 d\phi}, \quad (5)$$

where $\mathbf{x} = (x, y)$, $\mathbf{p} = (p_x, p_y)$, $\phi = (\phi_x, \phi_y)$. \bar{F} is the averaged smooth electron beam background distribution. We assume

$$\bar{F}(\mathbf{x}, \mathbf{p}, \eta; z) = \frac{e^{-\eta^2/(2\sigma_\eta^2)}}{(2\pi)^{3/2} \sigma_{p_x} \sigma_{p_y} \sigma_\eta} \exp\left(-\frac{x^2}{2\sigma_x^2} - \frac{(y - D\eta)^2}{2\sigma_y^2}\right) \exp\left(-\frac{p_x^2}{2\sigma_{p_x}^2} - \frac{p_y^2}{2\sigma_{p_y}^2}\right). \quad (6)$$

The electron beam density n_0 is given by $n_0 = \int d\eta dp_x dp_y \bar{F}(x, p, \eta; z)$, independent of z . n_0 is normalized such that when $D = 0$, i.e., before entering into the dispersion region, the peak density at $x = y = 0$ is n_0 , so $\int d\eta dp_x dp_y \bar{F}(0, 0, p_x, p_y, \eta; 0)|_{D=0} = 1$. We assume the electron beam in the undulator is approximately matched with constant betatron functions such that $\sigma_{p_x} = k_{\beta_x} \sigma_x = \sigma_x / \beta_x$, $\sigma_{p_y} = k_{\beta_y} \sigma_y = \sigma_y / \beta_y$, $p_x = \frac{dx}{dz}$, $p_y = \frac{dy}{dz}$. Here β represent betatron function and k_β is its inverse.

$A_\nu(\phi_x, \phi_y, z)$ is the angular representation of Fourier transform a_ν of the horizontal electric field component E at frequency $\omega = \nu\omega_1$, while the resonance harmonic frequency is $\omega_s = h\omega_1$ in Eq. (2), where $\omega_1 = 2\pi c/\lambda_1$ is the fundamental frequency for fundamental wavelength λ_1 . We have

$$E(x, y, z, t) = \frac{1}{\sqrt{2\pi}} \int e^{-i\Delta\nu k_u z} e^{-i\nu(k_1 z - \omega_1 t)} a_\nu(x, y, z) \omega_1 d\nu$$

$$A_\nu(\phi_x, \phi_y; z) = \frac{1}{\lambda^2} \int d\mathbf{x} a_\nu(\mathbf{x}, z) e^{ik(x\phi_x + y\phi_y)}, \quad (7)$$

where detuning from a harmonic frequency ω_s is given by $(\omega - \omega_s)/\omega_s = (\nu - h)/h = \Delta\nu/h$. The corresponding

wave number for frequency ω is $k = \omega/c = 2\pi/\lambda = \nu k_1$. Likewise, the undulator wave number is $k_u = 2\pi/\lambda_u$ for a given undulator period λ_u .

We assume the input radiation $a_\nu^{(0)}(x, y, z)$, the solution of the Maxwell equation in free space, is a Gaussian beam with frequency ν and Rayleigh ranges $z_{Rx} = \frac{\pi w_x^2}{\lambda}$ and $z_{Ry} = \frac{\pi w_y^2}{\lambda}$, where $w_x = 2\sigma_{rx}$ and $w_y = 2\sigma_{ry}$ are corresponding waist sizes in x and y , respectively; σ_{rx} and σ_{ry} are respective rms sizes of the input laser beam. Since the factor $A_\nu^{(0)} A_\nu^{*(0)}$ appears in both the numerator and the denominator of Eq. (5), we shall take the constant coefficients as 1 in $a_\nu^{(0)}(x, y, z)$ in G . In other words,

$$E(x, z) \sim a_\nu^{(0)}(x, y, z) \exp(-ikz) = \frac{1}{\sqrt{q_x(z)}} \frac{1}{\sqrt{q_y(z)}} \times \exp\left(-ik \frac{x^2}{2q_x(z)} - ik \frac{y^2}{2q_y(z)} - ikz\right),$$

for $q_x(z) = z + iz_{Rx}$, and $q_y(z) = z + iz_{Ry}$. Then Eq. (7) gives the angular representation of input radiation $A_\nu^{(0)}(\phi_x, \phi_y, 0)$ in Eq. (5) as follows:

$$A_\nu^{(0)}(\phi_x, \phi_y, z) = \frac{1}{\sqrt{\lambda}} \exp\left(ik(z + iz_{Rx}) \frac{\phi_x^2}{2}\right) \frac{1}{\sqrt{\lambda}} \exp\left(ik(z + iz_{Ry}) \frac{\phi_y^2}{2}\right) = A_\nu^{(0)}(\phi_x, \phi_y, 0) \exp\left(ikz \frac{\phi_x^2 + \phi_y^2}{2}\right),$$

$$\text{with } A_\nu^{(0)}(\phi_x, \phi_y, 0) = \frac{1}{\lambda} \exp\left(-kz_{Rx} \frac{\phi_x^2}{2} - kz_{Ry} \frac{\phi_y^2}{2}\right). \quad (8)$$

Thus, the angular divergence rms values are $\sigma_{\phi_x} = \sigma_{rx}/z_{Rx}$ and $\sigma_{\phi_y} = \sigma_{ry}/z_{Ry}$. Similarly, the undulator radiation amplitude in Eq. (5) is given by

$$U_\nu^*(\phi, \eta, \mathbf{x}, \mathbf{p}; z) = \int_{-L/2}^{L/2} ds e^{-ik\mathbf{x}\cdot\phi} e^{i \int_0^s ds_1 \xi_\nu(\phi, \eta, \mathbf{x}, \mathbf{p}; s_1)}$$

$$\text{where } \xi_\nu(\phi, \eta, \mathbf{x}, \mathbf{p}; s) = (\Delta\nu - 2\nu\eta)k_u + \nu \frac{2K_0^2}{2 + K_0^2} \alpha k_u y_0 + \frac{k}{2} ((p_{0x} - \phi_x)^2 + k_{\beta_x}^2 x_0^2 + (p_{0y} - \phi_y)^2 + k_{\beta_y}^2 y_0^2), \quad (9)$$

where $\mathbf{x}_0(s; \mathbf{x}, \mathbf{p})$, $\mathbf{p}_0(s; \mathbf{x}, \mathbf{p})$ are solutions of the equations of betatron equation of motion

$$\frac{dx_0}{ds} = p_{x0}, \quad \frac{dy_0}{ds} = p_{y0},$$

$$\frac{dp_{x0}}{ds} = -k_{\beta_x}^2 x_0, \quad \frac{dp_{y0}}{ds} = -k_{\beta_y}^2 y_0 \quad (10)$$

with the initial condition $\mathbf{x}_0(s=0; \mathbf{x}, \mathbf{p}) = \mathbf{x}$, $\mathbf{p}_0(s=0; \mathbf{x}, \mathbf{p}) = \mathbf{p}$. Here we neglect the focusing introduced by the gradient α , and we assumed the focusing comes from the natural focusing and the external focusing by quadrupole magnets and approximate the beta functions by constant values.

About Eq. (9) representing the FEL phase, for the introduction of the focusing terms $k_{\beta x}^2 x_0^2$, we refer to [23], as it is important for the development of Maxwell-Vlasov equations in high-gain FEL theory, in particular, this term allows the emittance condition $\epsilon < \frac{\lambda_x}{4\pi}$ to be relaxed for sufficient gain in the early design of LCLS, and it is also important for this paper itself. The derivation details can be found in, for example, Ref. [25]. The ϕ_x in $(p_{0x} - \phi_x)^2$ was introduced in Ref. [12] when Kim introduced the angular representation into the low gain formula.

The second term $\nu \frac{2K_0^2}{2+K_0} \alpha k_u y_0$ in Eq. (9) is related to the resonance condition [Eq. (4)], where αy represents the K value change due to the vertical gradient α and vertical displacement y in the transverse gradient undulator. This extra term is discussed in Ref. [5]. It represents the detuning due to the change of K value induced by the energy-correlated vertical displacement. The first term in Eq. (9) represents the detuning of the radiation and the detuning due to the energy spread η . Thus the first two terms combined represent the detuning due to the energy spread being compensated by the detuning due to the effect induced by the transverse gradient and vertical dispersion. We can see this compensation effect also in Eq. (4).

The constant $c_h = \frac{e^2 K^2 [JJ]_h^2 n_0}{8mc^2 \epsilon_0 \gamma^2 \lambda^2}$, where the electron beam density, n_0 , at the peak is determined by current $I = ec n_0 \Sigma = 2\pi \sigma_x \sigma_y ec n_0$ (the current of an approximately flat-top bunch with transverse Gaussian distribution). To write the gain G into a form convenient for scaling with h and λ_u , as shown in Eq. (1), we have (with Alfvén current $I_A = 4\pi mc^3 \epsilon_0 / e$)

$$c_h = \frac{I \pi K^2 [JJ]_h^2}{I_A \gamma^3} \frac{1}{4\pi \sigma_x \sigma_y \lambda^2}. \quad (11)$$

To calculate the gain G , we need to carry out the multi-variable integral in Eq. (5). Before the multivariable integration, the approach in [5,6] is to first take a “no focusing approximation” by neglecting the terms $k_{\beta x}^2 x_0^2 + k_{\beta y}^2 y_0^2$, following the step prescribed in [12]. With this approximation, a gain formula can be transformed into a form where the integrand becomes a convolution of the distribution function

$$\xi_\nu(\phi, \eta, \mathbf{x}, \mathbf{p}; s) = \xi_\nu^{(0)}(\eta, x, p; s) - k \mathbf{p}_0(s) \phi + \frac{k}{2} \phi^2,$$

$$\text{where } \xi_\nu^{(0)}(\eta, x, p; s) \equiv \xi_\nu(\phi = 0, \eta, \mathbf{x}, \mathbf{p}; s_1) = (\Delta\nu - 2\nu\eta)k_u + \nu \frac{2K_0^2}{2+K_0} \alpha k_u y_0 + \frac{k}{2} (p_x^2 + k_{\beta x}^2 x^2 + p_y^2 + k_{\beta y}^2 y^2). \quad (12)$$

with the radiation brightness and undulator brightness. This form is appropriate for a Gaussian integration which finally leads to a double integral convenient for numerical calculation.

The condition for neglecting $k_{\beta x}^2 x_0^2$ in $(p_{0x} - \phi_x)^2 + k_{\beta x}^2 x_0^2$, because p_x and $k_{\beta x} x$ are about the order of $k_{\beta x} \sigma_x$, corresponds to require $\sigma_{\phi x} \gg k_{\beta x} \sigma_x$. This condition becomes $\sigma_{\phi y} \gg k_{\beta y} \sigma_y$ in y . We found our optimization often leads to a set of parameters that violate this condition, in particular, when emittance is not very small and we need to increase k_β . In fact, in the example we developed in Sec. IV, for $\epsilon_{x0} = 80$ pm, the optimized $\beta_x = 6.6$ m and Rayleigh range $Z_{Rx} = 4$ m give $k_\beta \sigma_x / \sigma_{\phi x} \approx 2.3$.

Hence, we would like to try to take into account the effect of the betatron motion in the gain optimization without the limitation imposed by this condition. For a lattice of the undulator section with quasiuniform focusing and constant dispersion, we consider a segmented undulator interleaved with quadrupole doublets providing almost constant beta functions and dipole correctors next to the quadrupoles to keep the beam trajectory almost straight for an approximately constant dispersion in the transverse gradient undulator. We also need to include proper phasers to match the wavefront propagation through the segmented undulator. Although we have a preliminary example of such a lattice, this work is still in its early stage, and more studies are needed to work out all details and determine the tolerances for the deviation from constant beta functions and dispersion. This paper is only the first step in this direction, the detailed lattice design and study of its effects on the FEL performance is a separate R&D project, which is outside the scope of this article.

When the beta functions and dispersion are kept approximately constant, the beam transverse profile is approximately invariant along the undulator, and the interaction between the effects of the betatron motion, the dispersion, and the FEL embodied in the integral in Eq. (5) is significantly simplified. Under this circumstance, it turns out that without neglecting the focusing, the multiple integrals are still possible to be reduced to a double integral, mainly because the integrations over $x, p_x, y, p_y, \eta, \phi_x, \phi_y$ are all Gaussian in nature, as shown in Sec. III.

III. GAIN CALCULATION BY GAUSSIAN INTEGRATION

To write the integrand in Eq. (5) into a Gaussian integral, we first separate the variable ϕ in Eq. (9) as follows:

Because the last term in $\xi_\nu^{(0)}$ is invariant independent of s , \mathbf{x}_0 and \mathbf{p}_0 are replaced by their initial values \mathbf{x} and \mathbf{p} , and the only term dependent on s is $\nu \frac{2K_0^2}{2+K_0^2} \alpha k_u y_0(s)$. Since $\mathbf{x} + \int_0^s ds_1 \mathbf{p}_0(s) = \mathbf{x}_0(s)$, we have $U_\nu^*(\boldsymbol{\phi}, \eta, \mathbf{x}, \mathbf{p}; z) = \int_{-L/2}^{L/2} ds e^{-ik\mathbf{x}_0(s)\boldsymbol{\phi} + i\frac{k}{2}\boldsymbol{\phi}^2 s} e^{i \int_0^s ds_1 \xi_\nu^{(0)}(\eta, \mathbf{x}, \mathbf{p}; s_1)}$ in Eq. (9), so the gain in Eq. (5) becomes

$$G = -c_h I_{1e} \left(\int |A^{(0)}(\boldsymbol{\phi})|^2 d\boldsymbol{\phi} \right)^{-1},$$

where $I_{1e} \equiv \int \int \int d\eta d\mathbf{x} d\mathbf{p} \bar{F}(\mathbf{x}, \mathbf{p}, \eta; 0) \frac{\partial}{\partial \eta} \left| \int_{-L/2}^{L/2} ds I_{1r} e^{i \int_0^s ds_1 \xi_\nu^{(0)}(\eta, \mathbf{x}, \mathbf{p}; s_1)} \right|^2$

with $I_{1r}(s) \equiv \int d\boldsymbol{\phi} A^{(0)}(\boldsymbol{\phi}) e^{-ik\mathbf{x}_0(s)\boldsymbol{\phi} + i\frac{k}{2}\boldsymbol{\phi}^2 s}$. (13)

Substituting Eq. (8) into $I_{1r}(s)$ and using $x_0(s) = x \cos(\frac{s}{\beta_x}) + \beta_x p_x \sin(\frac{s}{\beta_x})$, $y_0(s) = y \cos(\frac{s}{\beta_y}) + \beta_y p_y \sin(\frac{s}{\beta_y})$ assuming the constant beta approximation, we find

$$I_{1r}(s) = -i \frac{1}{\sqrt{z_{Rx} - is} \sqrt{z_{Ry} - is}} \exp [c_x(s)x^2 + 2c_{xp}(s)xp_x + c_{px}(s)p_x^2] \exp [c_y(s)y^2 + 2c_{yp}(s)yp_y + c_{py}(s)p_y^2]$$

where $c_x(s) \equiv -k \frac{\cos^2(\frac{s}{\beta_x})}{2(z_{Rx} - is)}$, $c_{px}(s) \equiv -k \frac{\beta_x^2 \sin^2(\frac{s}{\beta_x})}{2(z_{Rx} - is)}$, $c_{xp}(s) \equiv -k \frac{\beta_x \cos(\frac{s}{\beta_x}) \sin(\frac{s}{\beta_x})}{2(z_{Rx} - is)}$,

$$c_y(s) \equiv -k \frac{\cos^2(\frac{s}{\beta_y})}{2(z_{Ry} - is)}$$
, $c_{py}(s) \equiv -k \frac{\beta_y^2 \sin^2(\frac{s}{\beta_y})}{2(z_{Ry} - is)}$, $c_{yp}(s) \equiv -k \frac{\beta_y \cos(\frac{s}{\beta_y}) \sin(\frac{s}{\beta_y})}{2(z_{Ry} - is)}$,
$$\left(\int |A^{(0)}(\boldsymbol{\phi})|^2 d\boldsymbol{\phi} \right)^{-1} = 2\pi w_x w_y,$$

$$I_{1e} = \int \int \int d\eta d\mathbf{x} d\mathbf{p} \bar{F}(\mathbf{x}, \mathbf{p}, \eta; 0) \frac{\partial}{\partial \eta} \int_{-L/2}^{L/2} \int_{-L/2}^{L/2} ds dz |I_{1r}(s) I_{1r}^*(z)| e^{i \int_0^s ds_1 \xi_\nu^{(0)}(\eta, \mathbf{x}, \mathbf{p}; s_1)} e^{-i \int_0^z ds_1 \xi_\nu^{(0)}(\eta, \mathbf{x}, \mathbf{p}; s_1)}. \quad (14)$$

Now substituting $\int_0^s ds_1 y_0(s)$ into Eq. (12), we get

$$\int_0^s ds_1 \xi_\nu^{(0)}(\eta, x, p; s_1) = (\Delta\nu - 2\nu\eta)k_u s + \frac{k}{2}(p_x^2 + k_{\beta_x}^2 x^2 + p_y^2 + k_{\beta_y}^2 y^2)s$$

$$+ \nu \frac{2K_0^2}{2 + K_0^2} \alpha k_u \beta_y y \left[\sin\left(\frac{s}{\beta_y}\right) - \sin\left(\frac{z}{\beta_y}\right) \right] - \nu \frac{2K_0^2}{2 + K_0^2} \alpha k_u \beta_y^2 p_y \left[\cos\left(\frac{s}{\beta_y}\right) - \cos\left(\frac{z}{\beta_y}\right) \right]. \quad (15)$$

Finally with $\frac{\partial}{\partial \eta} i \int_0^s ds_1 \xi_\nu^{(0)}(\eta, x, p, s_1) - \frac{\partial}{\partial \eta} i \int_0^z ds_1 \xi_\nu^{(0)}(\eta, x, p, s_1) = -2i\nu k_u (s - z)$, we have

$$I_{1e} = \int_{-L/2}^{L/2} \int_{-L/2}^{L/2} ds dz \int \int \int d\eta d\mathbf{x} d\mathbf{p} I_{1r}(s) I_{1r}^*(z) \bar{F}(\mathbf{x}, \mathbf{p}, \eta; 0) e^{i \int_0^s ds_1 \xi_\nu^{(0)}(\eta, \mathbf{x}, \mathbf{p}; s_1)} e^{-i \int_0^z ds_1 \xi_\nu^{(0)}(\eta, \mathbf{x}, \mathbf{p}; s_1)} (-2i\nu k_u)(s - z).$$

Collecting all the exponential factors in $I_{1r}(s) I_{1r}^*(z) \bar{F}(\mathbf{x}, \mathbf{p}, \eta; 0)$ and in $e^{i \int_0^s ds_1 \xi_\nu^{(0)}(\eta, \mathbf{x}, \mathbf{p}; s_1)}$, $e^{-i \int_0^z ds_1 \xi_\nu^{(0)}(\eta, \mathbf{x}, \mathbf{p}; s_1)}$ together [see Eqs. (6), (14), and (15)] and defining

$$D_R(s, z) \equiv \sqrt{z_{Rx} - is} \sqrt{z_{Ry} - is} \sqrt{z_{Rx} + iz} \sqrt{z_{Ry} + iz}, \quad (16)$$

we find

$$I_{1e} = \int_{-L/2}^{L/2} \int_{-L/2}^{L/2} ds dz \left(\frac{(-i2\nu k_u)(s-z) \exp[i\Delta\nu k_u(s-z)]}{D_R(s,z)} \frac{1}{(2\pi)^{3/2} \sigma_{px} \sigma_{py} \sigma_\eta} \right) I_x(s,z) I_{y\eta}(s,z),$$

where $I_x(s,z) = \iint dx dp_x \exp(-\Phi_x)$

and $I_{y\eta}(s,z) = \iint d\eta dy dp_y \exp(-\Phi_{y\eta})$ (17)

with

$$\begin{aligned} \Phi_x &= A_x x^2 + A_{px} p_x^2 + B_{xp} x p_x, \\ A_x &= \frac{1}{2\sigma_x^2} D_x, \quad D_x = 1 - 2\sigma_x^2 [c_x(s) + c_x^*(z)] - ikk_{\beta_x}^2 \sigma_x^2 (s-z), \\ A_{px} &= \frac{1}{2\sigma_{px}^2} D_{px}, \quad D_{px} = 1 - 2\sigma_{px}^2 [c_{px}(s) + c_{px}^*(z)] - ik\sigma_{px}^2 (s-z), \\ B_{xp} &= -2[c_{xp}(s) + c_{xp}^*(z)], \end{aligned}$$
 (18)

and

$$\begin{aligned} \Phi_{y\eta} &= A_\eta \eta^2 + A_y y^2 + A_{py} p_y^2 + B_{\eta y} y \eta + B_{yp} y \eta + B_\eta \eta + B_y y + B_{py} p_y, \\ A_\eta &\equiv \frac{1}{2\sigma_\eta^2} + \frac{D^2}{2\sigma_y^2}, \quad A_{py} \equiv \frac{1}{2\sigma_{py}^2} D_{py}, \quad D_{py} = 1 - 2\sigma_{py}^2 [c_{py}(s) + c_{py}^*(z)] - ik\sigma_{py}^2 (s-z), \\ A_y &\equiv \frac{1}{2\sigma_y^2} - [c_y(s) + c_y^*(z)] - i\frac{k}{2} k_{\beta_y}^2 (s-z), \\ B_{\eta y} &= -\frac{D}{\sigma_y^2}, \quad B_{yp} = -2[c_{yp}(s) + c_{yp}^*(z)], \quad B_\eta = 2i\nu k_u (s-z), \\ B_y &= -B_\alpha c_s(s,z), \quad B_{py} = B_\alpha \beta_y c_c(s,z), \quad B_\alpha \equiv i\nu \frac{2K_0^2}{2 + K_0^2} \alpha k_u \beta_y, \end{aligned}$$
 (19)

where $c_s(s,z) \equiv \left[\sin\left(\frac{s}{\beta_y}\right) - \sin\left(\frac{z}{\beta_y}\right) \right]$, $c_c(s,z) \equiv \left[\cos\left(\frac{s}{\beta_y}\right) - \cos\left(\frac{z}{\beta_y}\right) \right]$. (20)

Φ_x and $\Phi_{y\eta}$ are quadratic polynomials in x, p_x and in η, y, p_y , respectively. Their coefficients are functions of s, z only. By linear transformation, they can be transformed into diagonal quadratic form. Hence $I_x(s,z)$ and $I_{y\eta}(s,z)$ are Gaussian integrals. We give a brief description of the process of transforming to Gaussian integration in Appendix B. The result is

$$\begin{aligned} I_x &= \frac{2\pi \sigma_{px} \sigma_x}{\sqrt{(D_x D_{px} - \sigma_x^2 \sigma_{px}^2 B_{xp}^2)}}, \\ I_{y\eta} &= \frac{(2\pi)^{\frac{3}{2}} \sigma_\eta \sigma_y \sigma_{py}}{\sqrt{D_{py}} \sqrt{D_{\eta y}}} \exp\left(\frac{N_{\eta y}}{D_{\eta y}} \sigma_\eta^2 \sigma_y^2\right), \end{aligned}$$
 (21)

where $D_x, D_{px}, D_{py}, B_{xp}$ are given in Eqs. (18) and (19) and

$$\begin{aligned} D_{\eta y} &= 1 + (\sigma_y^2 + D^2 \sigma_\eta^2) \left(2A_y - \frac{1}{\sigma_y^2} - \frac{\sigma_{py}^2 B_{yp}^2}{D_{py}} \right), \\ N_{\eta y} &= C_{ss} c_s^2(s,z) + C_0 + C_s c_s(s,z) + C_{sc} c_s(s,z) c_c(s,z) + C_{cc} c_c^2(s,z) + C_c c_c(s,z). \end{aligned}$$
 (22)

The sinusoidal functions $c_s(s,z)$ and $c_c(s,z)$ are given by Eq. (19). Their coefficients in $N_{\eta y}(s,z)$ are also functions of s, z given by

$$\begin{aligned}
C_{ss} &= B_\alpha^2 A_\eta, & C_0 &= B_\eta^2 \left(A_y - \frac{B_{yp}^2}{4A_{py}} \right), & C_s &= B_\eta B_\alpha B_{\eta y}, \\
C_{sc} &= \frac{B_{yp} B_\alpha^2 \beta_y A_\eta}{A_{py}}, & C_{cc} &= \frac{B_\alpha^2 \beta_y^2}{A_{py}} \left(A_\eta A_y - \frac{1}{4} B_{\eta y}^2 \right), & C_c &= \frac{B_\eta B_\alpha B_{\eta y} B_{yp} \beta_y}{2A_{py}}.
\end{aligned} \tag{23}$$

With these provisions, we find the gain G as a double integral over s, z . First substituting Eq. (22) into Eq. (17) to find I_{1e} , then substituting I_{1e} , $(\int |A^{(0)}(\boldsymbol{\phi})|^2 d\boldsymbol{\phi})^{-1}$ from Eq. (14), and the constant c_h in Eq. (11) into Eq. (13), with $\nu \approx h$, we finally have

$$\begin{aligned}
G &= - \left(\frac{hK^2 [JJ]_h^2}{\lambda_u} \right) \left(\frac{I \pi^2}{I_A \gamma^3} \right) (2I_{3D}) \frac{2\pi w_x w_y}{\lambda^2}, \\
\text{with } I_{3D} &= \int_{-L/2}^{L/2} \int_{-L/2}^{L/2} ds dz \frac{-i(s-z) \exp[i\Delta\nu k_u(s-z)]}{\sqrt{(D_x D_{px} - \sigma_x^2 \sigma_{px}^2 B_{xp}^2)} \sqrt{D_{py}} \sqrt{D_{\eta y}}} \exp \left(\frac{N_{\eta y}}{D_{\eta y}} \sigma_\eta^2 \sigma_y^2 \right) \frac{1}{D_R(s, z)},
\end{aligned} \tag{24}$$

where $D_{\eta y}, N_{\eta y}$ are given by Eqs. (22) and (23). The coefficients in $D_{\eta y}, N_{\eta y}$ are expressed by the coefficients $A_\eta, A_y, A_{py}, B_\eta, B_\alpha, B_{\eta y}, B_{yp}, B_{xp}$ and D_x, D_{px}, D_{py} of the polynomial $\Phi_x, \Phi_{y\eta}$ in the Gaussian integral, as given by Eqs. (18) and (19). The expressions in these coefficients, $c_x(s), c_{xp}(s), c_{px}(s), c_y(s), c_{yp}(s), c_{py}(s)$, are given in Eq. (14). The sinusoidal functions $c_s(s, z), c_c(s, z)$ in $N_{\eta y}$ are given in Eq. (19).

Because of the effect of the betatron motion, the structure of the factors in I_{3D} is more complicated than the corresponding double integral in [5,6]. However, the numerical calculation of the double integral is simple, so it is appropriate for optimization.

As a check, in the 1D limit, $D_x = D_{px} = D_{py} = D_{\eta y} = 1, B_{xp} = 0, D_R(s, z) = z_{Rx} z_{Ry} = \frac{\pi^2 w_x^2 w_y^2}{\lambda^2}$. The radiation beam size is the same as the electron beam size $\sigma_{rx} = w_x/2 = \sigma_x, \sigma_{ry} = w_y/2 = \sigma_y$. If energy spread is negligible, $\sigma_\eta = 0$, we have

$$\begin{aligned}
I_{3D} &= \left(\int_{-L/2}^{L/2} \int_{-L/2}^{L/2} ds dz \{ -i(s-z) \exp[i\Delta\nu k_u(s-z)] \} \right) \\
&\quad \times \frac{\lambda^2}{\pi^2 w_x^2 w_y^2} \\
&= -L^3 \frac{1}{2} \frac{d}{d\Phi} \left(\frac{\sin \Phi}{\Phi} \right)_{\Phi=\Delta\nu k_u L/2}^2 \left(\frac{\lambda^2}{\pi^2 w_x^2 w_y^2} \right).
\end{aligned}$$

Then G becomes the G_{1D} given by Eq. (1).

IV. AN EXAMPLE OF GAIN CALCULATION

Equation (24) is the main result of this paper. As an example, we apply this formula to explore the possibility of a hard x-ray FEL oscillator for a light source at energy as low as 3 GeV and explore the required electron beam quality and undulator for an upgrade option of NSLS-II with an XFEL.

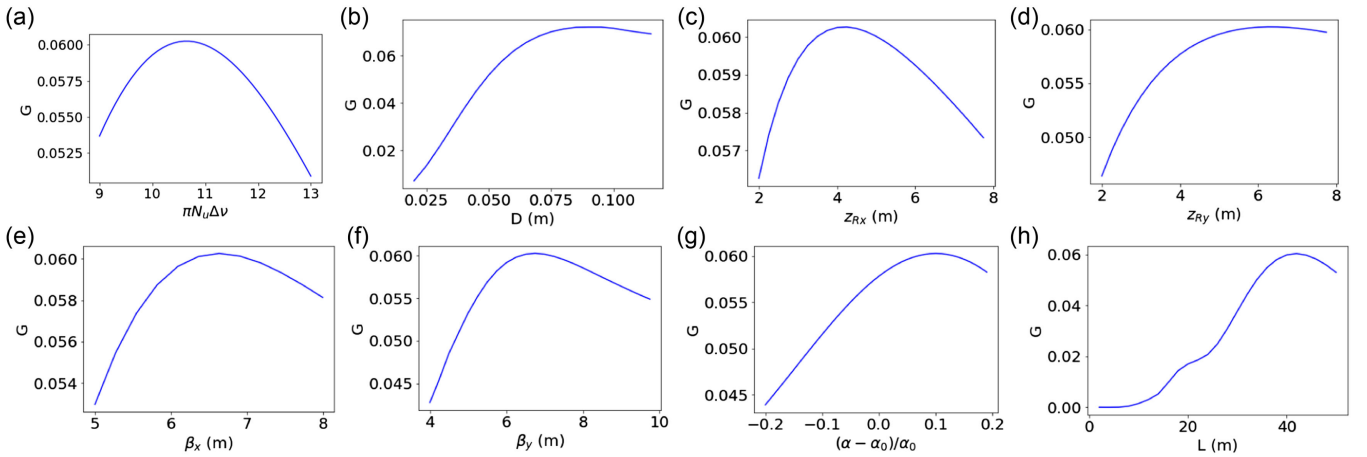


FIG. 3. Maximum gain resulted from the iterative scan of detuning (a) $\Delta\nu$, (b) vertical dispersion D , the input radiation Rayleigh ranges (c) z_{Rx} , (d) z_{Ry} , beta functions (e) β_x , (f) β_y , (g) the transverse gradient $(\alpha - \alpha_0)/\alpha_0$, and (h) the undulator length L . The variables were scanned one by one taking the optimal value from the previous variable scan. All of the figures except the last one are calculated at undulator length of 42 m where the gain reaches the maximum.

TABLE I. Parameters for maximum G .

E (GeV)	I (A)	λ_u (cm)	h	G (%)	K_0	ϵ_x (pm)	ϵ_y (pm)	D (m)	β_x (m)	β_y (m)	z_{Rx} (m)	z_{Ry} (m)	α (m ⁻¹)	σ_x (μ m)	σ_y (μ m)
3	73	2.26	5	6.0	1.29	80	1.7	0.05(V)	6.6	6.9	4.0	6.3	49	23	3.5

First, taking collective effects into account, we assume a 3 GeV FEL at 0.12 nm, approximate the bunch as a flattop pulse, and the current $I = 73A$ for a bunch length of 180 ps. For this example, we assume a local coupling correction in the undulator section to minimize the local vertical emittance and to blow up the vertical emittance in the rest of the ring for mitigation of the intrabeam scattering. The revolution period is about 2.6 μ s, so the bunch current is 5 mA. As discussed in Sec. I, we plot the first factor $\frac{K^2[JJ]_h^2}{\lambda_u}$ in the 1D gain formula as a function of λ_u in Fig. 1(a) and plot the gap g vs λ_u in Fig. 1(b). For $h = 5$, as a compromise between larger gain and gap, we choose $\lambda_u = 2.26$ cm and $\frac{K^2[JJ]_h^2}{\lambda_u} = 4.96$ m⁻¹, with gap $g = 7.5$ mm, $K_0 = 1.29$.

We assume the emittance $\epsilon_x = 80$ pm, $\epsilon_y = 1.7$ pm, energy spread $\sigma_\eta = 10^{-3}$, and undulator length $L = 42$ m and scan the seven variables: detuning $\Delta\nu$, dispersion D , focusing beta functions β_x , β_y , the input radiation Rayleigh ranges z_{Rx} , z_{Ry} , and the transverse gradient α to find maximum gain. During the scan, we find the transverse gradient α should be allowed to deviate from α_0 (where $\alpha_0 D = \frac{2+K_0^2}{K_0^2}$). Actually, we find the optimized α close but larger than α_0 .

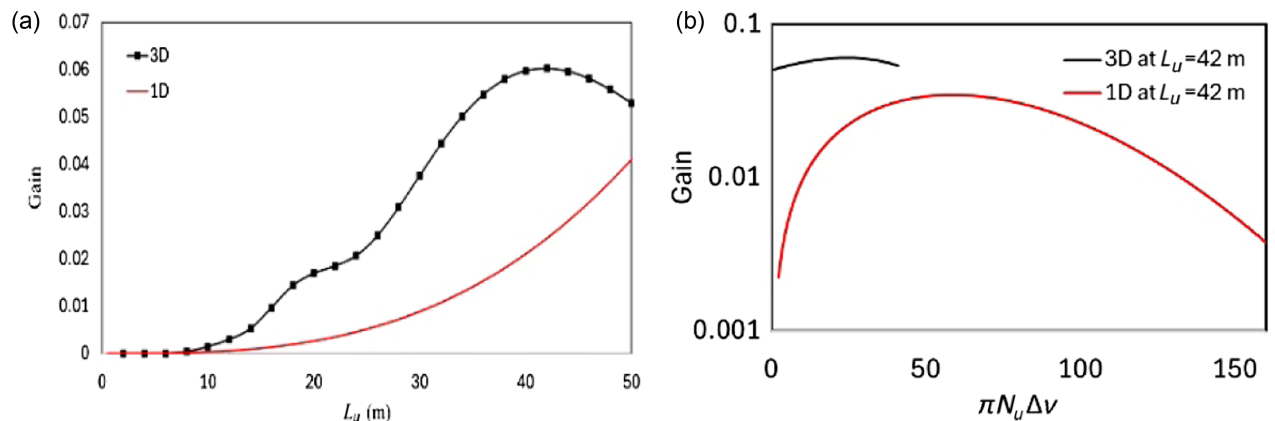
The plot of the scan in the last scan cycle is given in Fig. 3. The maximum gain is 7% in the last cycle for dispersion at 8 cm. However, we limit the vertical dispersion to 5 cm and the gain is 6.0%. In the subplot of G vs L , the maximum gain is reached at $L = 42$ m. The parameters for this setting are given in Table I. In Table I, the energy spread is $\sigma_\eta = 10^{-3}$, the undulator length is taken as $L = 42$ m, the x-ray wavelength is $\lambda_s = 0.12$ nm

and gap $g = 7.5$ mm. For dispersion D , (V) is vertical dispersion.

Although the vertical emittance of 1.7 pm seems quite small, it is within the achievable range for a fourth-generation synchrotron light source. A few projects already consider operations with the vertical emittance of the same order, e.g., for APS-U with 10% coupling, the vertical emittance is about 4 pm [26], and for Elettra 2.0, it is 2.5 pm with 1% coupling [27]. During the commissioning, ESRF-EBS demonstrated the measured vertical emittance below 1 pm with full coupling correction [28]. For a ring-based XFEL study assuming PETRA-IV parameters, the vertical emittance of 2.7 pm is considered [29]. Note that we consider the possibility of local coupling correction to provide 1.7 pm vertical emittance within the XFEL undulator section only.

We remark that no meaningful comparison can be made between the formula derived in this paper and other approximate formulas discussing higher harmonic gain under similar conditions. First, because the 3D no-focusing gain formula cited in the introduction does not consider higher harmonics, and second, because the 1D gain formula is too inaccurate and does not allow for comparison. However, in Fig. 4, we provide a comparison with the 1D gain using the same set of parameters in Fig. 3 and use this as a justification for the necessity for the newly derived 3D harmonic gain approximation.

The 1D gain does not take the diffraction and betatron oscillation into account; thus, it should be much larger than the 3D gain that considers those factors. However, when we added the effect of the energy spread, which is large for a storage ring, into the 1D gain estimation, the 1D gain became much smaller (3 orders' magnitude). Since in the

FIG. 4. 1D gain compared with 3D gain formula derived in this paper. (a) Gain vs L_u , (b) gain vs detuning at $L_u = 42$ m.

3D case, we apply the optimized transverse gradient scheme to mitigate the large energy spread of a storage ring, the 1D gain has become smaller than the 3D gain, as shown in Fig. 4. This can be understood via how the 1D and 3D gains are influenced differently by the detuning. Because of these, the 1D calculation can change between either very high gain or very small gain as we vary the different parameters, and none of the results can be trusted, let aside whether it will provide information about where the maximum gain is.

V. GAIN OPTIMIZATION WITH COLLECTIVE EFFECTS

As one can see in the previous section, XFELo requires quite a high peak beam current and small emittance. The emittance of synchrotron light sources has been continuously reduced in past decades. Implementation of the multibend achromat (MBA) technology resulted in the development of a new generation of synchrotrons with much lower emittance. Recently, three new MBA-based rings have been commissioned [30–32] and a few upgrade projects are being developed worldwide [26,27,33–36]. We consider an XFELo option for a lattice based on the recently developed complex bend approach for the future low-emittance upgrade of NSLS-II [37]. This lattice provides a horizontal emittance of 25 pm at a beam energy of 3 GeV fitting the present NSLS-II tunnel with a circumference of 792m. We propose to place the 42m long XFELo undulator in a straight section with a vertical dispersion bypassing 3 out of 30 achromat cells.

However, collective effects of beam dynamics significantly affect electron beam parameters in medium-energy (3–4 GeV) storage rings because the beams are small in all three dimensions and the particle density in the bunch is quite high. The main adverse effect impeding the achievement of the required combination of beam parameters is intrabeam scattering (IBS). To mitigate the collective effects, higher-harmonic rf cavities are used for bunch lengthening. The other strong intensity-dependent effect is the bunch lengthening due to potential well distortion by the longitudinal impedance of the vacuum chamber.

For a realistic assessment of a ring-based XFELo, we carried out multiparameter optimization of the FEL gain [Eq. (24)] assuming the vertical dispersion of 5 cm, emittance, energy spread, and bunch length determined by the lattice model taking into account the effect of IBS together with the impedance-driven bunch lengthening and higher-harmonic cavities. For the low-emittance synchrotrons, the light-generating insertion devices make a major contribution to the total energy loss per turn U_0 determining the radiation damping, so we include them in the lattice model. We optimized the detuning $\Delta\nu$, beta functions β_x, β_y , the input radiation Rayleigh ranges z_{Rx}, z_{Ry} , and the transverse gradient α to find the maximum gain. We optimized these six variables using a gradient-based method implemented in MATLAB [38] that is designed to work on problems

where the objective and constraint functions are both continuous and have continuous first derivatives.

We applied the high-energy approximation of the IBS theory [39]. The equilibrium emittance $\epsilon_{x,y}$ and relative energy spread σ_p are expressed as

$$\epsilon_{x,y} = \frac{\epsilon_{x0,y0}}{1 - \tau_{x,y}/T_{x,y}}, \quad \sigma_p^2 = \frac{\sigma_{p0}^2}{1 - \tau_p/T_p},$$

where $\epsilon_{x0,y0}$ and σ_{p0} are the emittance and energy spread, respectively, at zero beam current; τ_x, τ_y , and τ_p are the radiation damping times. T_{xy} and T_p are the IBS growth times given by

$$\frac{1}{T_p} \simeq \frac{r_0^2 c N}{32 \gamma^3 \epsilon_x \epsilon_y \sigma_s \sigma_p^2} \left(\frac{\epsilon_x \epsilon_y}{\langle \beta_x \rangle \langle \beta_y \rangle} \right)^{1/4} \ln \frac{\langle \sigma_y \rangle \gamma^2 \epsilon_x}{r_0 \langle \beta_x \rangle}, \quad (25)$$

$$\frac{1}{T_{x,y}} \simeq \frac{\sigma_p^2 \langle \mathcal{H}_{x,y} \rangle}{\epsilon_{x,y}} \frac{1}{T_p}, \quad (26)$$

r_0 is the classical electron radius, σ_s is the rms bunch length, σ_y is the vertical beam size, and $\mathcal{H}_{x,y}$ is the lattice function given by

$$\mathcal{H} = \beta_x \eta_x^2 + 2\alpha_x \eta_x \eta'_x + \gamma_x \eta_x^2, \quad (27)$$

where β_x is the amplitude function of betatron oscillation (beta function), $\alpha_x \equiv -\beta'_x/2$, $\gamma_x \equiv \frac{1+\alpha_x^2}{\beta_x}$, η_x and η'_x is the dispersion function and its derivative, respectively. As one can see, the IBS strongly depends on the beam energy, so its effect is not so significant for high-energy rings.

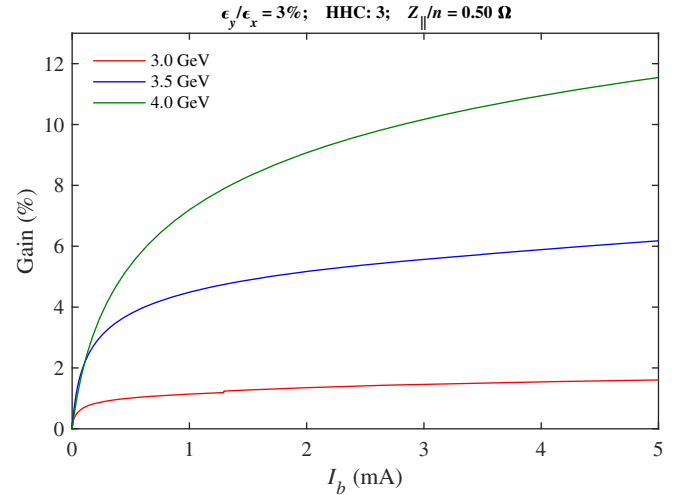


FIG. 5. FEL gain optimized for the beam energy of 3, 3.5, and 4 GeV, taking collective effects into account. Here, we assume a constant coupling of 3%, a factor of 3 bunch lengthening by a higher-harmonic cavity (HHC:3), and an inductive longitudinal impedance $Z_{||} = 0.5\Omega$.

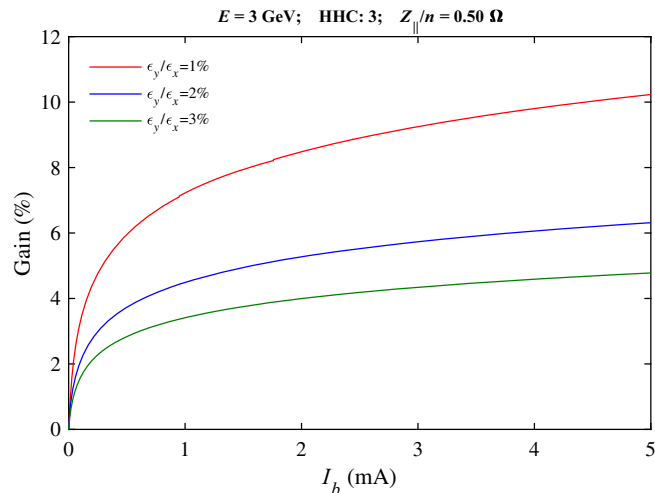


FIG. 6. FEL gain optimized for the beam energy of 3 GeV, taking collective effects into account. Here we assume a local coupling of 1%, 2%, and 3% in the undulator section and 100% everywhere else, a factor of 3 bunch lengthening by a higher-harmonic cavity (HHC:3), and an inductive longitudinal impedance $Z_{||} = 0.5 \Omega$.

The bunch lengthening caused by the beam interaction with the longitudinal impedance was calculated using the modified Zotter equation [40] in differential form. The effect of higher-harmonic cavities was simply modeled by a multiplication of the zero-intensity bunch length by a factor of 3.

As a result of the optimization, Fig. 4 shows the FEL gain as a function of single-bunch current for the beam energy of 3, 3.5, and 4 GeV and for a low coupling of 3%. With the constant coupling, the energy increases up to 3.5 GeV and, especially, up to 4 GeV results in a feasible gain of 6% and 11.5%, respectively, but the gain is too small (limited to within 2%) at 3 GeV and the XFEL looks unrealistic at this energy. However, there is a hope to make a 3 GeV XFEL feasible if it is possible to implement a local coupling correction reducing the vertical beam size only in the undulator section while keeping 100% coupling everywhere else in the ring to mitigate the intrabeam scattering. Although there is a theory developed a while ago [41] and a few simulation studies, e.g., [42], the local coupling correction is not a well-elaborated and widely used technique. So, the development of a realistic local correction scheme needs a separate intensive study, which is out of the scope of this article. We believe if a local coupling correction is implemented to reduce the vertical beam size only in the undulator section with coupling of 2% while keeping 100% coupling everywhere else in the ring, the XFEL looks feasible with gain reaching 6% even for 3 GeV energy. As one can see in Fig. 5, the gain at 4 GeV is much higher with the local 3% coupling (green curve) than the gain with global 3% coupling (red curve in Fig. 4) because of the significant mitigation of the intrabeam scattering by keeping large coupling outside the undulator section.

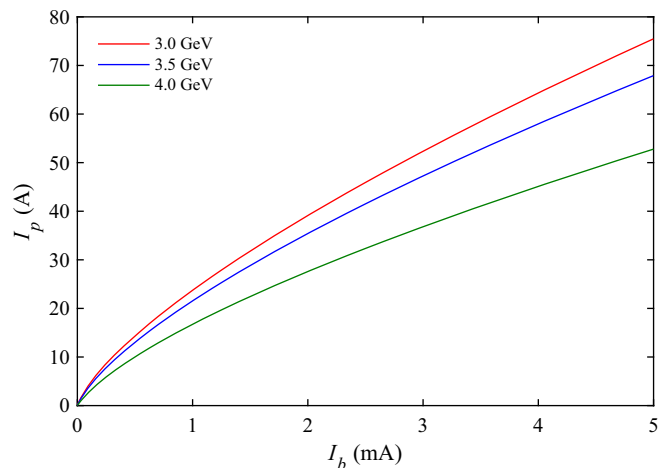


FIG. 7. Peak bunch current calculated for the beam energy of 3, 3.5, and 4 GeV, taking collective effects into account. Here we assume a factor of 3 bunch lengthening by a higher-harmonic cavity and an inductive longitudinal impedance $Z_{||} = 0.5 \Omega$.

We know the peak bunch current is more familiar for the FEL community, but here we plot the gain as a function of the single-bunch average current I_b because, in the ring case, the peak current $I_p = I_b \frac{\sqrt{2\pi} R_{\text{aver}}}{\sigma_s}$, where R_{aver} is the average radius of the ring, depends on the bunch length $\sigma_s(I_b)$ affected by collective effects, so it is not a constant. This dependence is nonlinear and varies with the energy, as shown in Fig. 6. So, it is not convenient to use the peak current as an independent variable. For the convenience of the readers in FEL community who maybe more familiar with peak current as an independent variable, we present a relation between peak current and average current in Fig. 7.

Although the gain shown in Figs. 4 and 5 is monotonically growing with the bunch current, especially at higher energies, one can see the slope is significantly decreasing at higher currents. So, we limited the single-bunch current to 5 mA and the total beam current to 50 mA assuming a uniform ten-bunch fill pattern, because a further increase of the beam intensity is not so efficient for the FEL gain and can be challenging due to shorter lifetime and possible collective instabilities.

VI. SUMMARY

We developed a gain formula for a hard x-ray FEL in the medium energy range between 3 and 4 GeV so that we do not need to take no focusing approximation in the calculation, in the hope this can be of use in exploring the possibility of x-ray FEL in this energy range. The formula allows gain calculation with harmonic lasing and strong focusing. We present an example to explore the limit of stringent conditions for an XFEL at the lowest possible energy. The example indicates hard x-ray FEL in 3 GeV is feasible, even though it sets rather challenging conditions for the storage ring parameters. The work presented here

justified our future effort to make a low-energy hard x-ray FEL possible. First, we need to develop numerical simulations to confirm the analytical calculation. For example, we need to use GENESIS code to confirm the gain calculation developed here, we need to develop a model for the lattice in the undulator section to check the tolerances for deviation from constant beta functions and dispersion, undulator errors, etc. The required small local emittance within the undulator section is the main challenge, we need to study nonlinear dynamics, coupling correction, and collective effects with extensive simulations and optimization for the storage ring lattice. We need to study whether the 1.7 pm local emittance is realistic, and if not, what would be the lowest energy that would make it realistic if we are not limited to 3 GeV. Actually, the 4 GeV option of the NSLS-II upgrade is not an impossible consideration either. In addition to these, we hope the approach of using harmonic lasing and strong focusing to lower the energy of hard x-ray FEL may be applied to other facilities. The optimization procedure taking harmonic number and focusing into account may also be applied to low-energy XFEL based on superconducting linac or maybe even high-gain single-pass XFEL. For higher energy XFEL (e.g., 6 to 8 GeV range), the optimization might also help to relax some stringent conditions on electron beam, undulator period, gap, etc.

ACKNOWLEDGMENTS

This work was supported by Brookhaven National Laboratory Directed Research and Development Program (Project 22-028) and by the U.S. Department of Energy (Contract No. DE-SC0012704).

APPENDIX A: OUTLINE OF DERIVATION OF FEL GAIN IN SMALL SIGNAL, LOW-GAIN REGIME

The FEL gain is derived from the coupled Maxwell-Vlasov equations, which initially was developed for high-gain FEL theory [21–24]. Later it is used for small gain FEL in [5,6,12]. We outline the gain formula derivation here as given in [12] in order to clarify the inclusion of the TGU, the dispersion, and we pay attention to the harmonic number $\nu \approx h$ in this paper. Many of the notations here have been introduced in Sec. II when we introduce the gain formula. The Maxwell equation in the notation here is

$$\delta F_\nu(\eta, \mathbf{x}, \mathbf{p}; z) = \delta F_\nu^{(0)}(\eta, \mathbf{x}, \mathbf{p}; z) - h_n \int_0^z ds a_\nu(x_0, s) \left(\frac{\partial}{\partial \eta} \bar{F}(\eta, \mathbf{x}_0(\mathbf{x}, \mathbf{p}, z; s), \mathbf{p}_0(\mathbf{x}, \mathbf{p}, z; s); s) \right) \times \exp \left(-2i\nu\eta k_u(s-z) + i\frac{\nu k_1}{2} \int_z^s dz_1 w[\mathbf{x}_0(\mathbf{x}, \mathbf{p}, z; z_1), \mathbf{p}_0(\mathbf{x}, \mathbf{p}, z; z_1)] + i\nu k_u \frac{K_0^2}{1 + \frac{K_0^2}{2}} \alpha \int_z^s dz_1 y_0 \right), \quad (\text{A4})$$

where $\delta F_\nu^{(0)}(\eta, \mathbf{x}, \mathbf{p}; z)$ is the solution without FEL interaction, related to the spontaneous radiation and will be neglected in the small gain calculation, and $\mathbf{x}_0(\mathbf{x}, \mathbf{p}, z; s)$, $\mathbf{p}_0(\mathbf{x}, \mathbf{p}, z; s)$ are solutions of the betatron motion [Eq. (10)] with an initial condition such that at $s = z$, $\mathbf{x}_0(\mathbf{x}, \mathbf{p}, z; s = z) = \mathbf{x}$, and $\mathbf{p}_0(\mathbf{x}, \mathbf{p}, z; s = z) = \mathbf{p}$.

$$\left(\frac{\partial}{\partial z} - i\Delta\nu k_u + \frac{i}{2k} \nabla_\perp^2 \right) a_\nu(x, z) = -g_n \int d\eta \int d\mathbf{p} \delta F_\nu(\eta, \mathbf{x}, \mathbf{p}; z), \quad (\text{A1})$$

where $g_n = \frac{eK[JJ]_h n_0}{4\epsilon_0 \gamma \omega_1}$ and $n_0 F(z, \theta, \eta, \mathbf{x}, \mathbf{p}) = k_1 \sum \delta(\eta - \eta_j) \delta(\mathbf{x} - \mathbf{x}_j) \delta(\mathbf{p} - \mathbf{p}_j) \delta(\theta - \theta_j)$ is the electron beam distribution function, $\theta = (k_1 + k_u)z - \omega_1 \bar{t}$ is the microbunching phase, and \bar{t} is the time of electron passing through z averaged over a period of the undulator. The function F is separated into two parts $F = \bar{F} + \delta F$, \bar{F} is the averaged smooth electron beam background distribution in Eq. (6) and δF is the deviation from \bar{F} including shot noise in the beam and the microbunching due to FEL interaction. $\delta F_\nu(z, \theta, \eta, \mathbf{x}, \mathbf{p})$ is the Fourier transform of δF :

$$\delta F_\nu(\eta, \mathbf{x}, \mathbf{p}; z) = \frac{1}{\sqrt{2\pi}} \int e^{i\nu\theta} \delta F(z, \theta, \eta, \mathbf{x}, \mathbf{p}) d\theta. \quad (\text{A2})$$

The Vlasov equation is essentially the Liouville theorem applied to perturbation theory in a small signal regime. After Fourier transform from θ to ν , it is in the form

$$\left(\frac{\partial}{\partial z} + \dot{\theta} \frac{\partial}{\partial \theta} + \dot{\mathbf{x}} \frac{\partial}{\partial \mathbf{x}} + \dot{\mathbf{p}} \frac{\partial}{\partial \mathbf{p}} \right) \delta F_\nu(\eta, \mathbf{x}, \mathbf{p}; z) = -h_h a_\nu(\mathbf{x}, z) \frac{\partial}{\partial \eta} \bar{F}(\eta, \mathbf{x}, \mathbf{p}; z), \quad (\text{A3})$$

where the Fourier transformed energy equation is $\frac{1}{\sqrt{2\pi}} \int \dot{\eta} e^{i\nu\theta} d\theta = -h_h a_\nu(x, y, z)$, with $h_h = \frac{e\omega_1 K[JJ]_h}{2mc^2 \gamma^2}$, \dot{x}, \dot{p} are given by betatron motion [Eq. (10)], and the phase equation is

$$\dot{\theta} = \frac{d\theta}{dz} = k_u \left(2\eta - \frac{K_0^2}{1 + \frac{K_0^2}{2}} \alpha y \right) - \frac{k_1}{2} w(\mathbf{x}, \mathbf{p}),$$

$$\text{where } w(\mathbf{x}, \mathbf{p}) \equiv p_x^2 + k_{\beta x}^2 x^2 + p_y^2 + k_{\beta y}^2 y^2.$$

To solve the coupled Maxwell-Vlasov equations with two unknowns $a_\nu(x, z)$ and δF_ν , we eliminate the unknown δF_ν by first solving the Vlasov equation [Eq. (A3)] to express δF_ν in terms of $a_\nu(x, z)$. Treating this linear partial differential equation as a one variable linear ordinary differential equation with δF_ν as a function of z , using the ‘‘method of variation of constants,’’ the result is

Inserting Eq. (A4) into the Maxwell equation [Eq. (A1)] and neglecting the first term which contributes to the spontaneous radiation, we get the field equation for $a_\nu(\mathbf{x}, z)$

$$\left(\frac{\partial}{\partial z} - i\Delta\nu k_u + \frac{i}{2k}\nabla_\perp^2\right)a_\nu(\mathbf{x}, z) = -g_n h_n \int d\eta \int d\mathbf{p} \int_0^z ds \bar{F}(\eta, \mathbf{x}_0(s), \mathbf{p}_0(s); s) \frac{\partial}{\partial \eta} a_\nu(\mathbf{x}_0(s), s) \\ \times \exp\left(-2i\nu\eta k_u(s-z) + i\frac{k}{2}\int_z^s dz_1 w[\mathbf{x}_0(z_1), \mathbf{p}_0(z_1)] + i\nu k_u \frac{K_0^2}{1 + \frac{K_0^2}{2}} \alpha \int_z^s dz_1 y_0(z_1)\right). \quad (\text{A5})$$

We abbreviate $\mathbf{x}_0(\mathbf{x}, \mathbf{p}, z; s)$ as $\mathbf{x}_0(s)$, and similarly for $\mathbf{p}_0(s)$. $\mathbf{x}, \mathbf{p}, z$ in the argument is implied, and $k = \nu k_1$. The version of this equation with the transverse gradient $\alpha = 0$ has been used as a dispersion relation [23] to derive the gain length formula including the effect of finite emittance, diffraction, and betatron focusing on the development in the high-gain regime for the first time.

Later, this equation was applied to solve for small gain regime [5,6,12]. Applying the transform $\frac{1}{\lambda^2} \int d\mathbf{x} e^{ik(x\phi_x + y\phi_y)}$ in Eq. (7) to both sides of Eq. (A5) converts it to a field equation for $A_\nu(\phi_x, \phi_y; z)$ given by

$$\left(\frac{\partial}{\partial z} - i\Delta\nu k_u - \frac{ik}{2}\phi^2\right)A_\nu(\phi; z) = b(z) \\ \text{where } b(z; \phi) = -\frac{1}{\lambda^2} g_n h_n \int d\eta d\mathbf{p} \int d\mathbf{x} \int d\phi' \exp\left(\Delta\nu k_u z + i\frac{k}{2}\phi^2 z\right) \bar{F}(\eta, \mathbf{x}, \mathbf{p}; z) \quad (\text{A6})$$

$$\times \frac{\partial}{\partial \eta} e^{ik\mathbf{x}\phi} \exp\left[-i\int_0^z dz_1 \xi_\nu(\phi, \eta, \mathbf{x}, \mathbf{p}; z_1)\right] \int_{-L/2}^z ds_1 e^{-ik\mathbf{x}\phi'} \exp\left[i\int_0^{s_1} dz_1 \xi_\nu(\phi', \eta, \mathbf{x}, \mathbf{p}; z_1)\right] A_\nu(\phi', 0) \\ \text{and } \xi_\nu(\phi', \eta, \mathbf{x}, \mathbf{p}; z_1) = (\Delta\nu - 2\nu\eta)k_u + \nu k_u \frac{K_0^2}{1 + \frac{K_0^2}{2}} \alpha y_0(z_1) + \frac{k}{2} w(\mathbf{x}_0(z_1), \mathbf{p}_0(z_1) - \phi). \quad (\text{A7})$$

The input radiation $A_\nu^{(0)}(\phi_x, \phi_y, z)$ in Eq. (7), the Gaussian beam, is the solution of this equation with $b(z)$ set to zero. When substituting $A_\nu^{(0)}(\phi_x, \phi_y, 0)$ as $A_\nu(\phi', 0)$ into Eq. (A6) first-order perturbation, the equation is considered as a linear ordinary differential equation with z as variable and $b(z)$ as the inhomogeneous term, the solution at the end $z = L/2$ is

$$A_\nu(\phi; L/2) = A_\nu^{(0)}(\phi; L/2) + A_\nu^{(1)}(\phi, L/2) \\ \text{with } A_\nu^{(0)}(\phi; L/2) = \exp\left(i\Delta\nu k_u L/2 + \frac{ik}{2}\phi^2 L/2\right) A_\nu^{(0)}(\phi', 0), \\ A_\nu^{(1)}(\phi) = -\frac{1}{\lambda^2} g_n h_n \exp\left(i\Delta\nu k_u L/2 + \frac{ik}{2}\phi^2 L/2\right) \int d\eta d\mathbf{p} \int d\mathbf{x} \int d\phi' \bar{F}(\eta, \mathbf{x}, \mathbf{p}; 0) \\ \times \frac{\partial}{\partial \eta} \int_{-L/2}^{L/2} ds e^{ik\mathbf{x}\phi} \exp\left(-i\int_0^s dz_1 \xi_\nu(\phi, \eta, \mathbf{x}, \mathbf{p}; z_1)\right) \int_{-L/2}^s ds' e^{-ik\mathbf{x}\phi'} \exp\left(i\int_0^{s'} dz_1 \xi_\nu(\phi', \eta, \mathbf{x}, \mathbf{p}; z_1)\right) A_\nu(\phi', 0). \quad (\text{A8})$$

Here $\bar{F}(\eta, \mathbf{x}, \mathbf{p}; z)$ in Eq. (A6) has been replaced by $\bar{F}(\eta, \mathbf{x}, \mathbf{p}; 0)$ because it is independent of z . In Eq. (A8), and in Eq. (5) of Sec. II, the $\mathbf{x}_0(s; \mathbf{x}, \mathbf{p}), \mathbf{p}_0(s; \mathbf{x}, \mathbf{p})$ in $\xi_\nu(\phi', \eta, \mathbf{x}, \mathbf{p}; z_1)$ are solutions of the equations of betatron motion Eq. (10) with the initial condition.

The gain is defined as

$$G = \frac{\int (|A_\nu(\phi; L/2)|^2 - |A_\nu^{(0)}(\phi; L/2)|^2) d\phi}{\int |A_\nu^{(0)}(\phi; L/2)|^2 d\phi} \\ \approx \frac{\int (A_\nu^{(0)*}(\phi; L/2) A_\nu^{(1)}(\phi, L/2) + \text{c.c.}) d\phi}{\int |A_\nu^{(0)}(\phi; L/2)|^2 d\phi}, \quad (\text{A9})$$

where the term of the second power of $\frac{1}{\lambda^2} g_n h_n$ is neglected. Upon substituting Eq. (A8) with Eq. (A9), we arrive at the gain formula of Eq. (5).

APPENDIX B: GAUSSIAN INTEGRAL OF SEVERAL VARIABLES

We brief on the calculation of the three variable Gaussian integrals $I_{y\eta}$ in Eq. (21) of Sec. III. The integral I_x is a two-variable Gaussian and can be considered a simplified version of $I_{y\eta}$. The exponent in $I_{y\eta}(s, z) = \int \int d\eta dy dp_y \exp(-\Phi_{y\eta})$ is

$$\Phi_{y\eta} = A_\eta \eta^2 + A_y y^2 + A_{py} p_y^2 + B_{\eta y} \eta y + B_{yp} y p_y + B_{\eta\eta} \eta + B_{yy} y + B_{py} p_y, \quad (\text{B1})$$

where the coefficients are given by Eq. (19). The first step is to transform the coefficients of the three quadratic terms

to 1 by a transform $A_\eta \Rightarrow A_\eta / \sqrt{A_\eta}$, $y \Rightarrow y / \sqrt{A_y}$, $p_y \Rightarrow p_y / \sqrt{A_{py}}$ so

$$I_{y\eta} = \frac{1}{\sqrt{A_\eta A_{py} A_y}} \int \int d\eta dy dp_y \exp(-\Phi_{y\eta 1})$$

$$\Phi_{y\eta 1} = \eta^2 + p_y^2 + y^2 + d\eta y + cyp_y + a\eta + by + gp_y,$$

where $a = \frac{B_\eta}{\sqrt{A_\eta}}$, $b = \frac{-B_y}{\sqrt{A_y}} [\sin(\frac{s}{\beta_y}) - \sin(\frac{z}{\beta_y})]$, $B_\alpha \equiv i\nu \frac{2K_0^2}{2+K_0^2} \times \alpha k_u \beta_y$, $c = \frac{B_{yp}}{\sqrt{A_{py} A_y}}$, $d = \frac{B_{\eta y}}{\sqrt{A_\eta A_y}}$, and $g = \frac{B_{\eta y}}{\sqrt{A_{py} A_y}} [\cos(\frac{s}{\beta_y}) - \cos(\frac{z}{\beta_y})]$.

Next, we shift the origin to the maximum of $\Phi_{y\eta 1}$ at η_0, p_{y0}, y_0 by a transform $\eta \Rightarrow \eta + \eta_0$, $p_y \Rightarrow p_y + p_{y0}$, $y \Rightarrow y + y_0$, which is found by solving three linear equations. The result is

$$I_{y\eta} = \frac{1}{\sqrt{A_\eta} \sqrt{A_{py}} \sqrt{A_y}} \exp\left(-\frac{4b^2 + a^2(4-c^2) - 4abd - 4bcg + (4-d^2)g^2 + 2acd g}{4(4-c^2-d^2)}\right) \int \int d\eta dy dp_y \exp(-\Phi_{y\eta 2})$$

$$\Phi_{y\eta 2} = X^T \cdot m \cdot X = \eta^2 + p_y^2 + (\eta d + c p_y) y + y^2$$

$$\text{where } X = \begin{pmatrix} \eta \\ p_y \\ y \end{pmatrix}, \quad m = \begin{pmatrix} 1 & 0 & \frac{d}{2} \\ 0 & 1 & \frac{c}{2} \\ \frac{d}{2} & \frac{c}{2} & 1 \end{pmatrix}.$$

$\Phi_{y\eta 2}$ is in quadratic form and can be transformed into diagonal quadratic form using the eigenvectors V of the matrix m

$$V = \begin{pmatrix} -\frac{c}{d} & -\frac{d}{\sqrt{c^2+d^2}} & \frac{d}{\sqrt{c^2+d^2}} \\ 1 & -\frac{c}{\sqrt{c^2+d^2}} & \frac{c}{\sqrt{c^2+d^2}} \\ 0 & 1 & 1 \end{pmatrix}. \quad (\text{B2})$$

Now apply transform: $X \Rightarrow VX$ with determinant $\det(V) = \frac{2\sqrt{c^2+d^2}}{d}$ to obtain

$$I_{y\eta} = \frac{1}{\sqrt{A_\eta A_{py} A_y}} \frac{2\sqrt{c^2+d^2}}{d} \exp\left(\frac{4b^2 + a^2(4-c^2) - 4abd - 4bcg + (4-d^2)g^2 + 2acd g}{4(4-c^2-d^2)}\right) \times \int \int d\eta dy dp_y \exp\left(-\left(1 + \frac{c^2}{d^2}\right)\eta^2 - \left(2 - \sqrt{c^2+d^2}\right)p_y^2 - \left(2 + \sqrt{c^2+d^2}\right)y^2\right).$$

The integrals over η, y , and p_y are separately carried out, and finally, with a, b, c, d , and g substituted and rearranged, the result is Eq. (21).

- [1] L. H. Yu, Gain of hard X-ray FEL at 3 GeV and required parameters, in *Proceedings of IPAC-2021, Campinas* (2021).
- [2] T. I. Smith, J. M. J. Madey, L. R. Elias, and D. A. G. Deacon, Reducing the sensitivity of a free-electron laser to electron energy, *J. Appl. Phys.* **50**, 4580 (1979).
- [3] N. Kroll, P. Morton, M. Rosenbluth, J. Eckstein, and J. Madey, Theory of the transverse gradient wiggler, *IEEE J. Quantum Electron.* **17**, 1496 (1981).
- [4] Panagiotis Baxevanis, Yuantao Ding, Zhirong Huang, and Ronald Ruth, 3D theory of a high-gain free-electron laser based on a transverse gradient undulator, *Phys. Rev. ST Accel. Beams* **17**, 020701 (2014).
- [5] R. R. Lindberg *et al.*, Transverse gradient undulators for a storage ring X-ray FEL oscillator, in *Proceedings of FEL2013, New York, NY* (JACoW, Geneva, Switzerland, 2013), paper THOBNO02, p. 740.
- [6] Y. S. Li, R. Lindberg, and K.-J. Kim, Optimization of the transverse gradient undulator (TGU) for application in a storage ring based XFEL, in *Proceedings of the 39th Free Electron Laser Conference, FEL2019, Hamburg, Germany* (JACoW, Geneva, Switzerland, 2019).
- [7] K.-J. Kim, L. Assoufid, F.-J. Decker, Z. Huang, R. R. Lindberg, G. Marcus, T. O. Raubenheimer, X. Shi, D. Shu, Yu. Shvyd'ko *et al.*, Test of an x-ray cavity using double-bunches from the LCLS Cu-Linac, in *Proceedings of 10th International Particle Accelerator Conference, IPAC-2019, Melbourne, Australia* (JACoW, Geneva, Switzerland, 2019), pp. 1887–1890, [10.18429/JACoW-IPAC2019-TUPRB096](https://doi.org/10.18429/JACoW-IPAC2019-TUPRB096).
- [8] P. Rauer *et al.*, Cavity based x-ray free electron laser demonstrator at the European X-ray Free Electron Laser facility, *Phys. Rev. Accel. Beams* **26**, 020701 (2023).
- [9] N.-S. Huang *et al.*, The MING proposal at SHINE: Megahertz cavity enhanced X-ray generation, *Nucl. Sci. Tech.* **34**, 6 (2023).
- [10] Zhirong Huang and Kwang-Je Kim, *Phys. Rev. E* **62**, 7295 (2000).
- [11] E. A. Schneidmiller and M. V. Yurkov, Harmonic lasing in x-ray free electron lasers, *Phys. Rev. ST Accel. Beams* **15**, 080702 (2012).
- [12] K.-J. Kim, *Nucl. Instrum. Methods Phys. Res., Sect. A* **318**, 489 (1992).
- [13] K. Halbach, *J. Phys. (Paris), Colloq.* **44**, C1 (1983), [https://scholar.google.com/scholar?q=K.+Halbach,+J.+Phys.+Paris,+Colloq.+44,+C1+\(1983\)&hl=en&as_sdt=0&as_vis=1&oi=scholar](https://scholar.google.com/scholar?q=K.+Halbach,+J.+Phys.+Paris,+Colloq.+44,+C1+(1983)&hl=en&as_sdt=0&as_vis=1&oi=scholar).
- [14] K.-J. Kim and Y. V. Shvyd'ko, *Phys. Rev. ST Accel. Beams* **12**, 030703 (2009).
- [15] A. Snigirev, V. Kohn, I. Snigireva, and B. Lengeler, A compound refractive lens for focusing high-energy x-rays, *Nature (London)* **384**, 49 (1996).
- [16] G. Tiwari *et al.*, Compound refractive lenses for X-rays, Brookhaven National Laboratory Report No. BNL-225130-2023-TECH/NSLSII-ASD-TN-398, 2023.
- [17] R. Margraf *et al.*, Low-loss stable storage of 1.2 Å X-ray pulses in a 14 m Bragg cavity., *Nat. Photonics* **17**, 878 (2023).
- [18] G. Marcus *et al.*, Cavity-based free-electron laser research and development: A Joint Argonne National Laboratory and SLAC National Laboratory Collaboration, in *Proceedings of the 39th Free Electron Laser Conference, FEL2019, Hamburg, Germany* (JACoW, Geneva, Switzerland, 2019).
- [19] Y. Shvyd'ko, S. Stoupin, V. Blank, and Sergey Terentyev, Near-100% Bragg reflectivity of X-rays. *Nat. Photonics* **5**, 539 (2011).
- [20] G. Tiwari *et al.*, Power loss analysis for optical cavity of X-ray free-electron laser oscillator at 10 KeV, Brookhaven National Laboratory Report No. BNL-225541-2024-TECH, 2024 and Optica Open. Preprint, [10.1364/opticaopen.25691697.v2](https://doi.org/10.1364/opticaopen.25691697.v2).
- [21] J. M. Wang and L. H. Yu, *Nucl. Instrum. Methods Phys. Res., Sect. A* **250**, 484 (1986).
- [22] S. Krinsky and L. H. Yu, *Phys. Rev. A* **35**, 3406 (1987).
- [23] L. H. Yu, S. Krinsky, and R. L. Gluckstern, *Phys. Rev. Lett.* **64**, 3011 (1990).
- [24] L. H. Yu, *Phys. Rev. A* **44**, 5178 (1991).
- [25] A. He, L. Yang, and L. H. Yu, High-gain free-electron laser theory, introduction, in *Synchrotron Light Sources and Free-Electron Lasers* (Springer, Cham, 2020), https://link.springer.com/referenceworkentry/10.1007/978-3-030-23201-6_2.
- [26] Advanced Photon Source Upgrade Project, Final Design Report, 2019, APSU-2.01-RPT-003, <https://publications.anl.gov/anlpubs/2019/07/153666.pdf>.
- [27] E. Karantzoulis, Elettra 2.0—The diffraction limited successor of Elettra, *Nucl. Instrum. Methods Phys. Res., Sect. A* **880**, 158 (2018).
- [28] P. Raimondi *et al.*, The Extremely Brilliant Source storage ring of the European Synchrotron Radiation Facility, *Commun. Phys.* **6**, 82 (2023).
- [29] Y. Li, R. Lindberg, and K.-J. Kim, Transverse gradient undulator in a storage ring X-ray free electron laser oscillator, *Phys. Rev. Accel. Beams* **26**, 030702 (2023).
- [30] P. Tavares *et al.*, Commissioning and first-year operational results of the MAX IV 3 GeV ring, *J. Synchrotron Radiat.* **25**, 1291 (2018).
- [31] L. Torino *et al.*, Beam instrumentation performances through the ESRF-EBS commissioning, in *Proceedings of 9th International Beam Instrumentation Conference, IBIC-2020, Santos, Brazil* (JACoW, Geneva, Switzerland, 2020), paper MOAO04.
- [32] L. Lin, Sirius accelerators overview, in *Proceedings of EIC, Sirius Commissioning, Liu Lin – IPAC'20, Caen, France, 2020* (2020), <https://indico.cern.ch/event/949203/contributions/3989688/attachments/2118546/3564877/EIC-Sirius.pdf>.
- [33] C. Steier *et al.*, Status of the conceptual design of ALS-U, in *Proceedings of 8th International Particle Accelerator Conference, IPAC-2017, Copenhagen, Denmark* (JACoW, Geneva, Switzerland, 2017), paper WEPAB104.
- [34] Y. Jiao *et al.*, The HEPS project, *J. Synchrotron Radiat.* **25**, 1611 (2018).
- [35] Diamond-II: Conceptual Design Report, 2019, <https://www.diamond.ac.uk/dam/jcr:ec67b7e1-fb91-4a65-b1ce-f646490b564d/Diamond-IIConceptualDesignReport.pdf>.
- [36] S. Shin, Lattice design and beam dynamics studies for fourth-generation stage ring, in *International Conference on Accelerators and Beam Utilization (ICABU2019), Daejeon, Korea, 2019* (2019), <https://indico.ibs.re.kr/event/307/>.

- [37] F. Plassard, G. Wang, T. Shaftan, V. Smaluk, Y. Li, and Y. Hidaka, Simultaneous correction of high order geometrical driving terms with octupoles in synchrotron light sources, *Phys. Rev. Accel. Beams* **24**, 114801 (2021).
- [38] MATLAB fmincon—Nonlinear optimization, <https://www.mathworks.com/help/optim/ug/fmincon.html>.
- [39] K. Bane *et al.*, Intrabeam scattering analysis of ATF beam measurements, SLAC National Accelerator Laboratory Report No. SLAC-PUB-8875, 2001.
- [40] B. Zotter, Potential-well bunch lengthening, CERN, the European Organization for Nuclear Research, Geneva, Switzerland, Report No. CERN SPS/81-14 (DI), 1981.
- [41] E. A. Perevedentsev, Combinations of skew-quadrupoles for local coupling control, in *Proceedings of the 7th European Particle Accelerator Conference, Vienna, Austria, 2000* (EPS, Geneva, 2000), pp. 1066–1068.
- [42] L. O. Dallin, Local transverse coupling control, in *Proceedings of the 19th Particle Accelerator Conference, Chicago, IL, 2001* (IEEE, Piscataway, NJ, 2001), pp. 2677–2679.